COBEM 2021 26th International Congress of Mechanical Engineering
ABCM Associação Brasileira de Engenharia e Ciências Mecânicas
November 22-26, 2021, Virtual Congress, Brazil

COB-2021-0888
MODELING AND SIMULATION OF A SMALL SIZE ROBOT KICKING MECHANISM

Reynaldo Santos de Lima
Autonomous Computational Systems Lab (LAB-SCA), Computer Science Division, Aeronautics Institute of Technology, São José dos Campos - SP, Brazil
reynaldo.sdlima@gmail.com

Daniela Vacarini de Faria
Embraer S.A., São José dos Campos - SP
danivacarini@gmail.com

Luiz Carlos Sandoval Góes
Aeronautics Institute of Technology, Praça Marechal Eduardo Gomes, 50 - Vila das Acacias, São José dos Campos - SP
goes@ita.br

Marcos Ricardo Omena de Albuquerque Maximo
Autonomous Computational Systems Lab (LAB-SCA), Computer Science Division, Aeronautics Institute of Technology, São José dos Campos - SP, Brazil
maximo.marcos@gmail.com

Abstract. *In this paper, we present the mathematical modeling and design of a kicking device for Small Size League robots. The modeling was based on energy flow analysis of different domains, as the system is a solenoid with moving ferromagnetic plunger and, therefore, non-constant inductance. The plunger's movement (mechanical system) is damped, retained with an elastic, and has its movement driven by a force resulting from the electrical current on the solenoid. On the other hand, the current flowing in the solenoid (electrical system) depends on the position of the plunger inside the solenoid, as a result of the influence on the solenoid's inductance. Thus, it is highlighted how magnetic interaction bonds the mechanical and electrical systems with a bond-graph, using a transducer common to this type of system. It is also noted that, for the studied model, the solenoid coil length (on the moving direction) is wider than the plunger, which provides a constant inductance for a short interval of time. These considerations and deductions are, finally, resumed in a system of ordinary differential equations. The mathematical model constructed was then simulated with numerical integration in MATLAB Simulink, highlighting the speed that a ball is expected to have after its collision with the moving solenoid plunger as a function of the amount of time the electrical circuit remained active. The parameters used for the integration are listed, some of which are design values of components and others are assumptions based on similar situations to the studied model and expected undesired effects, such as Columbian friction. The result is compared with three data points, usual options used in game to kick the ball, showing a good prediction by the model. In summary, the contribution of this work is providing a mathematical model of the kicking device which we expect to be more clear around energy transference between systems than previous models.*

Keywords: *Solenoid, kicking mechanism, modeling, robotics, electromechanical device.*

1. INTRODUCTION

The Small Size League (SSL) is a category within the RoboCup competition, which aims to promote the development of robotics and artificial intelligence. This league consists of a soccer match between two teams of six (in Division B) to eight (Division A) players each. This work focuses on a Division B scenario and rules. Each player is an omnidirectional robot with a maximum size of 15 cm in diameter. Each player is allowed to have both low and high kick mechanisms, provided that the kicked ball leaves the robot with a maximum velocity of 6.5 m/s (RoboCup, 2020).

Traditionally, a solenoid valve is used for these mechanisms, since it is capable of quickly delivering a great amount of energy and is easier to handle compared to other energy storage devices, such as springs or pneumatic valves (Zandsteeg, 2005). An electric solenoid may be inspected as a transducer, bonding electric and mechanical energy sources. To do so, it is constructed with a long coil and a ferromagnetic plunger – ideally soft in a magnetic perspective – and free to move inside the coil. Thus, a dynamic electromechanical system is a possible model – while the electrical system depends on

the plunger position, the mechanical system is disturbed by a force (from magnetic interaction) that drags the plunger forwards (Karnopp *et al.*, 2012; Fitzgerald *et al.*, 2003).

Developing a solenoid for an SSL robot, then, consists in understanding the influence of major electrical, as the wire diameter and its resistance, and mechanical, as elastic and damping constants influence, parameters and adjusting these for the project constraints, nonetheless obtaining a desired result. Thereby, consistent design in the solenoid parameters implies in better control over the speed that the ball is propelled, suiting a range of different strategies – from a simple pass to a shoot (Zickler *et al.*, 2009).

Regarding the development presented in this paper, we notice some works develop a similar physical model as ours, while considering approximations to the electrical current with respect to the time. Meessen *et al.* (2010) uses a constant current value, while focusing on a more rigorous analysis for experimental data. Zolanvari *et al.* (2015)presents similar modeling as us, but they approximate the current curve with time as linear to keep the model analytic.

Furthermore, some works present a simplified model, analysing solely the magnetic field generated by the kicking mechanism (Allali *et al.*, 2019). Finally, there is work made with an analogous approach for the model and simulation, but they stumbles on a model discontinuity (Demarchi *et al.*, 2018), a problem which we discuss in the current work, presenting an alternative to the analysis.

In this paper, we present the mathematical modeling and design of such a mechanism, as part of the SSL project of the robotics team ITAndroids. Despite modeling the kicking mechanism of an SSL robot is not novel, to the best of our knowledge, this work is the first one to do such modeling without approximations regarding the progress of the current with time to facilitate the analysis. As described in Section 3., our contribution lies in providing a mathematical model of the kicking device which we expect to be more accurate than previous models. Moreover, the developed model presents a concise energy flow analysis through the bond graph representation of the system, which provides an overview of the mechanism independent of the energy domain (electrical or mechanical).

The remaining of this paper is organized as follows. Section 2. develops the model proposed for the kicking mechanism, presenting the electrical characteristics (such as the circuit and the model for the solenoid's inductance) in Subsection 2.1 , the mechanical in Subsection 2.2 and joining both through energy flow analysis and variables adjustment in Subsection 2.3 . With the model fully developed, we present the numerical simulation through Simulink and its results in Section 3.. In Subsection 3.1 we focus on the simulation itself and the implementation enviroment; as for Subsection 3.2 , we show the results of this simulation, comparing them with a limited set of data obtained experimentally with one SSL robot.

2. MODELING THE KICKING MECHANISM

The Solenoid Kicking Mechanism used in robot soccer in the SSL is an electromechanical dynamical system constituted of two main subsystems: an RLC circuit and a mechanical impulsion system. First we develop both subsystems separately, then we connect those with a bond graph analysis. Bond graphs are a great tool in order to couple systems from different energy domains, which is the case of the current analysis. Therefore, we make references to some basic concepts, such as ports (connections between elements), capacitive, inertia, and resistance elements (each of these has a known correspondent for a specific energy domain) (Karnopp *et al.*, 2012; Fitzgerald *et al.*, 2003).

The electric system is a circuit made of a resistor, a capacitor, and an inductor, all associated in series (Alonso and Finn, 2014) (inertial electric port). The mechanical impulsion system is a capacitance mechanical port. These subsystems connect with each other through energy flow. The coupling occurs through an *IC* port (*I* stands for the inductance component in the electric circuit, while *C*, the damping mechanical system), while the interface of the energy transmission happens through the magnetic flow variance (Karnopp *et al.*, 2012).

Through this initial analysis, it is appropriate to distinguish the most important attributes in each subsystem. Then, we may proceed to the general (regarding the energy domain) approach of the system with a bond graph diagram analysis, from which we may extract a set of dynamics equations that accurately represents the model.

2.1 Energy Supply: RLC Circuit Analysis

To control the kick speed, an SSL robot manipulates the amount of time that the RLC circuit will be active. Based on that, it is fundamental to understand this energy supply occurring in the correspondent electronic supply board, which implies half the equations used to describe the dynamic system (see Section 3.).

The electronic board increases the input voltage from the energy source (a voltage source or battery) to a desired value (from a usual 11 V from the battery to a value higher than 150 V), from which a capacitor is charged. The capacitor discharge generates the current required for the RLC circuit. Thereby, describing the circuit outlined in Fig. 1, we obtain:

$$i(t) = -\frac{dq(t)}{dt}, \tag{1}$$

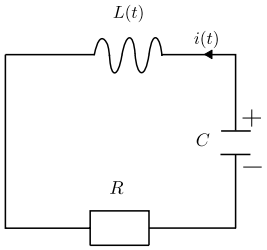

Figure 1. RLC circuit diagram with current $i(t)$ and inductance $L(t)$, both functions of time.

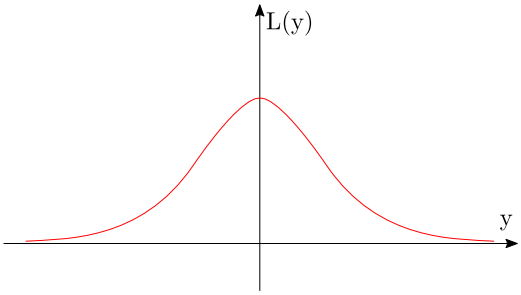

Figure 2. Inductance as a function of the position of the ferromagnetic plunger. In this figure the general case is illustrated, remaining some general characteristics, with $y = 0$ acting as an axis of symmetry.

$$0 = -\frac{q(t)}{C} + Ri(t) + \frac{d}{dt}[L(t)i(t)] = -\frac{q(t)}{C} + Ri(t) + L(t)\frac{di(t)}{dt} + i(t)\frac{dL(t)}{dt}, \tag{2}$$

where, in Eq. (1), $q(t)$ is the amount of charge the capacitor stores at time t, C is the capacitance of the circuit and $i(t)$ is the current through the circuit. Furthermore, in Eq. (2), R stands for the resistance in the circuit (coming mostly from the solenoid coil) and $L(t)$ is the time-varying inductance.

From this analysis, we must obtain $L(t)$ to fully describe the equations. In a solenoid, the inductance is a function of the time while there is a ferromagnetic plunger moving inside it. Figure 2 shows a general plot of inductance as a function of the position $L(y)$ (we assume zero position when the plunger is completely within the solenoid). Figure 3 shows an illustration of the moving plunger inside the solenoid.

The model consists of the analysis of flux linkage (λ) on a solenoid, which is described in Eq. (3).

$$\lambda(t, y) = i(t)L(y). \tag{3}$$

We first find the total reluctance, assuming, yet, the solenoid to be covered by a ferromagnetic material, whose reluctance is neglected (Cheung *et al.*, 1993). Using the magneto-motive force relationship with flux linkage, we obtain:

$$N^2 i(t) = \left(\frac{L_0 - |y|}{m\mu_0\mu_r A} + \frac{D - L_0 + |y|}{\mu_0 A}\right)\lambda, \tag{4}$$

where A stands for the section area of the solenoid; μ_0 is the magnetic permeability of vacuum; μ_r is the relative magnetic permeability of the ferromagnetic plunger; D is the total solenoid length; and N is the number of wire turns of the solenoid. It is also noted that the x in Fig. 3 has a direct relation to y, while the later is relative to the wall, and the first is the mechanical coordinate.

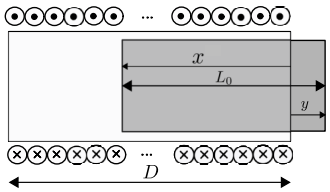

Figure 3. Illustration of a solenoid with a moving plunger in a cross section. In this figure the y component is illustrated, as is the main dimension of the solenoid, D.

From Eq. (4) we may obtain the inductance as a function of the ferromagnetic plunger position:

$$L(y) = \frac{N^2}{\frac{L_0-|y|}{\mu_0\mu_r A} + \frac{D-L_0+|y|}{\mu_0 A}}. \tag{5}$$

Equation (5) may be written at this point as a function of x, as x is the mechanical displacement and is related to y by:

$$y = x - L_0,\ 0 \leq x \leq L_0, \tag{6}$$

$$y = x - D, x \geq D. \tag{7}$$

Using Eq. (6) and (7) in Eq. (5), we may represent the inductance $L(x)$, as follows:

$$L(x) = \begin{cases} \frac{N^2}{\frac{x}{\mu_0\mu_r A} + \frac{D-x}{\mu_0 A}}, & 0 \leq x < L_0, \\ \frac{N^2}{\frac{L_0}{\mu_0\mu_r A} + \frac{D-L_0}{\mu_0 A}}, & L_0 \leq x < D, \\ \frac{N^2}{\frac{D+L_0-x}{\mu_0\mu_r A} + \frac{x-L_0}{\mu_0 A}}, & x \geq D. \end{cases} \tag{8}$$

Notice that the factor μ_r of ferromagnetic materials tends to be greater than 10^3 (Oxley *et al.*, 2009), which makes possible to the denominator in Eq. (5) to reach near zero while y reachs zero, as D is not longer than 10^{-1} m. In Fig. 2 it is seen a general case of Eq. (5), where is possible to observe a high peak when $y = 0$. This would represent a discontinuity in the model. Therefore, for this work, we consider the case where the plunger is smaller than the solenoid, and $-L_0 < y < L_0$, where L_0 is the plunger's length and $L_0 < D$ (see Fig. 3).

Thus, in the complete movement of the plunger, the inductance goes from an initial low value, when $y < 0$, increases until the whole plunger is completely inside the solenoid, then it finally leaves the solenoid, following a symmetrical movement from the beginning, with $y > 0$. For the transitory moment, when the whole plunger is inside the solenoid, we assume a simplified model where the magnetic force is constant and agrees with the value from $y = 0$.

2.2 Mechanical System

At this point, we have a consistent analysis of the Electric Energy Source, powered by batteries through the electronic power board; Furthermore, the magnetic circuit described in Eq. (4) is the main key to understand the transition of this electric energy to a mechanical form, an IC port – see Sec. 2.3. At some time t, we have an associated $x(t)$ and, as seen in Fig. 3, there will be some force (with magnetic source) F_m that drags the plunger proportionally to to the inductance derivative of $L(x)$ with relation to x.

To obtain F_m, we may use Magnetic Energy (or the Co-energy) derivative in relation to x (portion of the plunger that is outside the solenoid). We have $W_{fld}(\lambda, x)$ as the magnetic energy (Karnopp *et al.*, 2012; Fitzgerald *et al.*, 2003):

$$W_{fld}(\lambda, x) = \frac{1}{2}\frac{\lambda^2}{L(x)}. \tag{9}$$

Therefore:

$$F_m = -\frac{\partial W_{fld}(\lambda, x)}{\partial x} = \frac{\lambda^2}{2L(x)^2}\frac{\partial L(x)}{\partial x}. \tag{10}$$

To understand and describe F_m, we must study the energy flow as a function of x, which is made in Sec. 2.3. Aside from the solenoid, the mechanical system is constituted of a spring, with elastic constant k and initial displacement δ_0, and we assume the system to have (due to metallic contact) a viscous damping, with damping constant b. As there is contact between two aluminum surfaces (Barrett, 1990) (with respect to the parts that support the system to align the kick), a F_C factor is also added, from Colombian friction. Therefore, we will use a bond graph diagram analysis to describe the whole system.

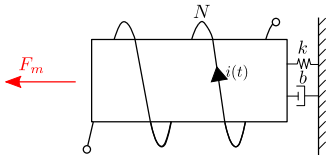

Figure 4. In this Figure, we may see a representation of the kicking system of an SSL Robot.

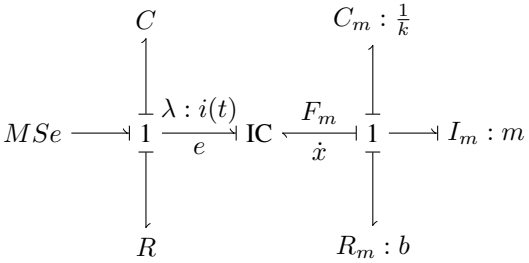

Figure 5. Bond graph representation of the Kicking System of an SSL Robot, as sketched in figures 1 and 3, where MSe stands for modulated source of effort and represents the voltage provided by the capacitor.

2.3 Bond Graph Diagram to the System

The Electromechanical System described in subsections 2.1 and 2.2 is represented in Fig. 4. The ferromagnetic plunger is surrounded by the solenoid wire, which terminals are connected to an RLC circuit (as in Fig. 1), composing a solenoid, whose inductance is a function of the plunger position $L(y)$. The solenoid has N turns throughout its whole area (partly filled with air, part with the moving plunger). As mentioned, there is a spring (constant k) and a viscous damping element (constant b). As the plunger moves and the current $i(t)$ flows through the coil, the force F_m drags the plunger.

Moreover, we will represent the system shown in Fig. 4 via bond graph, see Fig. 5, which allow us to equate the problem in terms of a Mechanical, x, and an Electromagnetic, λ, flux variable. In Fig. 5, e is assumed as the voltage on the capacitor (capacitance C), the effort variable at the circuit. Besides, C_m, I_m and R_m stands for the capacitance, the inertia and the resistance analogous of the mechanical system, respectively, with their parameters indicated. Finally, m represents the plunger mass.

From the bond graph in Fig. 5, we may observe the main systems described in this paper. The IC element represents the solenoid itself, as it works bonding the electrical port, in the left, and the mechanical port, in the right. Those bonds work with two type-1 junctions, as illustrated, where above the arrows directly connected to IC are electrical and mechanical flow variables – which represent charge flow and displacement flow, respectively.

Thus, the bond graph representation of the system enlightens the main system variables, with which we may obtain the differential form of the energy flow (IC-field transducer), as follows, where $W_{fld}(x, \lambda)$ represents the amount of magnetic stored energy (Fitzgerald *et al.*, 2003), W_{elec} is the electrical energy input, and W_{mech} is the mechanical energy output:

$$dW_{fld}(x, \lambda) = dW_{elec} - dW_{mech} = i(t)d\lambda - F_m dx. \tag{11}$$

From Eq. (9) and Eq. (3), we may represent the analogous of Eq. (10), regarding $L(x)$ as a function of x. Besides, with the bond graph in Fig. 5 we may describe dynamic equations from flow and effort values properties associated with type-1 junctions (Karnopp *et al.*, 2012).

Analyzing figures 1 and 4 and the energy associations represented via Bond graph in Fig. 5, we may obtain the following equations, that along with Eq. (1) and Eq. (2) are enough to fully describe the mechanism (with enough initial conditions given) at a given time:

$$\dot{x} = \frac{dx}{dt}, \tag{12}$$

$$m\frac{d\dot{x}}{dt} = \frac{\lambda^2}{2}\frac{L'(x)}{L(x)^2} - k(x - \delta_0) - b\dot{x} - F_c. \tag{13}$$

At this point, we have a set of equations with electric and mechanical variables dependent on time. Equations (1) and (12) may seem redundant at first, but these functions point how we may obtain the flux related variables – as pointed in Eq. (9) – of the system. Accordingly, we obtain from those relations a dynamic system from which we may build up a computer simulation.

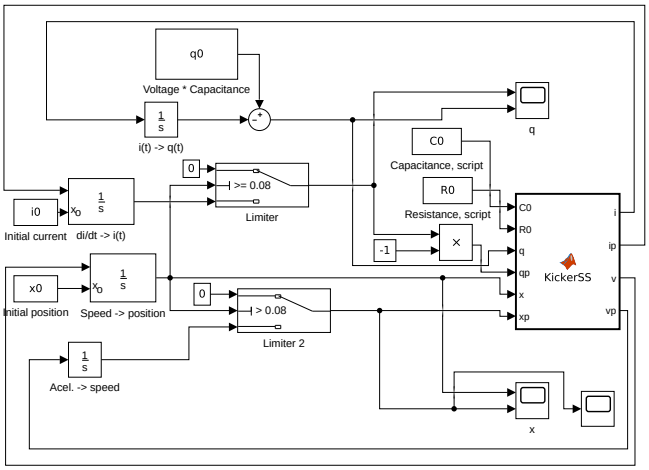

Figure 6. MATLAB Simulink environment. Blocks diagram of the simulation developed in this work.

3. SIMULATION RESULTS

With the whole system described and the relations of electrical and mechanical variables, we are able to construct a numerical simulation and compare its results with real experiments, as described in the following.

3.1 Simulation with *Simulink* and MATLAB

In order to make clear flow variables of the system we rewrite the set of described equations, where v stands for speed, as:

$$i(t) = -dotq(t), \tag{14}$$

$$\dot{i}(t) = \frac{q(t)}{CL(x)} - i(t)\frac{R}{L(x)} - v(t)\frac{L'(x)}{L(x)}i(t), \tag{15}$$

$$v(t) = \dot{x}, \tag{16}$$

$$\dot{v}(t) = \frac{i(t)^2 L'(x)}{2m} - \frac{k}{m}(x - \delta_0) - \frac{b}{m}v(t) - \frac{F_C}{m}. \tag{17}$$

Applying Eq. (14) to Eq. (17) with the values of electric and mechanical constants (related to an SSL Robot), and considering initial values $x(0)$, $v(0)$, $q(0)$ and $i(0)$, we may follow the plunger motion with numerical integration. Thereby, Fig. 6 shows a simulation within the MATLAB's Simulink environment intended to follow the movement proposed at a given time interval.

The simulation used automatic configurations regarding step size and type (fixed or variable step), with well behaved results. We are releasing our simulation model as open source for the community, in link `https://gitlab.com/itandroids/open-projects/ssl-kicking-mechanism-simulator`.

The blocks in Fig. 6 represent an operation within the simulation. The main block is a MATLAB function (KickerSS) that updates each major system variable by iteration, applying the dynamic system described in (14) to Eq. (17). Besides, each parameter used (see Tab. 1) affects output values and are used at some point in the simulation

The main variables from Fig. 6 are `x`, `xp`, `vp`, `q`, `i` and `ip`, each of them represents, respectively, the variables $x(t)$, $v(t)$, $\dot{v}(t)$, $q(t)$, $i(t)$ and $\dot{i}(t)$.

3.2 Validation using Real Data

Throughout the description of the proposed model within this paper, a set of parameters have been used to equate the kicking mechanism dynamic system. The values used in the simulation, part of our team's Small Size project, are stated in Tab. 1.

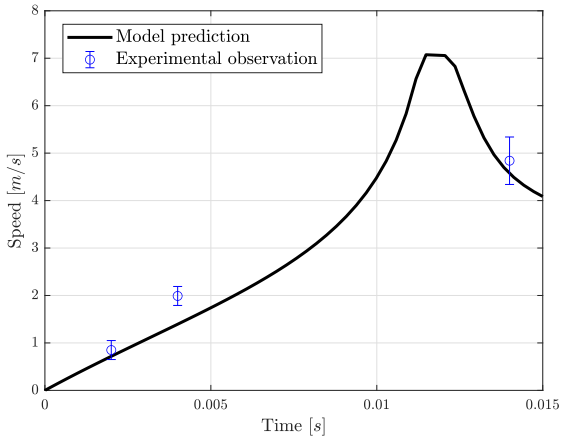

Figure 7. Solenoid plunger's speed over time as of the simulation, compared to a set of experimental values.

Furthermore, to describe the real system there is a limit to the plunger position that must be taken into account while comparing simulation to the real system behavior. This happens as the solenoid plunger has a hard stop restraining the plunger inside the robot's kicking mechanism. Through the proposed simulation, we may obtain the plunger's speed before reaching its position limit, thus enlightening the amount of time the circuit may be operating to obtain the desired speed.

Using the registered data exported from the simulation we may observe the output of velocity over time – representing the solenoid plunger speed, as presented in Fig. 7. Moreover, we analyzed three options of kicks in an SSL robot, each of them considered with a given time interval as input (time in which the kicking circuit is switched on) and the associated speed of the plunger as output – see Tab. 2.

To obtain the values in Tab. 2, we measured the ball speed for a set of kicks performed by a robot. The kicks were recorded and later the motion of the ball was tracked. Then, to estimate the final solenoid plunger's speed, the collision between the ball and the kicker was considered elastic, thus, the speed in Tab. 2 is estimated for the plunger. The error stated is obtained through the data's standard deviation.

As it is possible to gather comparing results from Fig. 7, we may observe that the simulation is relatively accurate for smaller values of activation time. It is possible to observe the plateau in speed, as the model reaches the point when the plunger is supposed to be fully within the solenoid.

It is important to notice that our model predicts the final plunger's speed within the RLC circuit actuation. Therefore, it is expected that the speed that the plunger reaches the ball is lesser than the presented in Fig. 7, as there is still an amount of time when mechanical forces are actuating alone. This shall result in slightly different results, as the magnetic force is considerably higher than the mechanical ones. Regardless, as it is still reliable, the model prediction in Fig. 7 is of great importance to choose the system's parameters and to search for the optimum value for the desired output speed, and, thus, the amount of time needed to be commanded in the robot's code.

Table 1. Kicking mechanism parameters.

Parameter	**Meaning**	**Value**
N	Number of coil turns	632
μ_0	Magnetic permeability of free space	$4\pi 10^{-7}\ T \cdot m$
μ_r	Relative magnetic permeability of the solenoid coil	1000
A	Section area	$\pi(6 \cdot 10^{-3})^2\ m^2$
R	Electric resistance	$10\ \Omega$
C	Electric capacitance	$2700\ \mu F$
k	Spring elastic constant	$20\ N/m$
δ_0	Spring's initial disp.	0
m	Ferromagnetic coil mass	$55\ g$
F_C	Coloumbian friction	$0.755\ N$
b	Damping constant	$0.5 \cdot 10^{-4}\ kg/s$

Table 2. Experimental tests for an SSL Robot Kick showing the Period of time the circuit is active (left) and the plunger's speed (right).

Time in $10^{-3}s$	**Speed in m/s**
2	0.85 ± 0.20
4	1.99 ± 0.20
14	4.84 ± 0.50

4. CONCLUSIONS

In this paper we developed a dynamic system model through a bond graph diagram for an SSL Kicking mechanism, applying it to a mathematical simulation within the Simulink environment with satisfactory results that can point which parameters are rather more effective to change while looking to obtain a desired speed for each kick. Furthermore, we observed that the proposed inductance function in Eq. (4) is not the best model when it comes to the plunger position totally inside the solenoid, proposing a constant substitute for this situation to obtain a symmetrical result for the inductance.

The work shows a reliable estimation, when comparing the simulation with experimental results, while providing an interesting overview of similar works developed in the RoboCup Small Size community. For future work, we expect to better model the transition phase, when the steel plunger is almost completely inside the solenoid, and gather experimental results for different times to obtain the complete experimental curve for Fig. 7.

5. ACKNOWLEDGEMENTS

Reynaldo Santos de Lima would like to thank Brazilian National Council for Scientific and Technological Development (CNPq) for his undergraduate research scholarship. The team ITAndroids would like to thank its sponsors: Altium, Cenic, Intel, ITAEx, Mathworks, Metinjo, Micropress, Polimold, Rapid, Solidworks, ST Microelectronics, WildLife, and Virtual Pyxis.

6. REFERENCES

Allali, J. *et al.*, 2019. "Namec - team description paper small size league robocup 2019 application of qualifcation in division b". Technical report, Universite de Bordeaux, France.

Alonso, M. and Finn, E.J., 2014. *Física: um curso universitário*, Vol. 1. Edgard Blücher, 2nd edition.

Barrett, R.T., 1990. *Fastener Design Manual*. Reference Publication 1228.

Cheung, N., Lim, K. and Rahman, M., 1993. "Modelling a linear and limited travel solenoid". pp. 1567–1572.

Demarchi, A., Farçoni, L., Pinto, A., Lang, R., Romero, R. and Silva, I., 2018. "Modelling a solenoid's valve movement". In H. Akiyama, O. Obst, C. Sammut and F. Tonidandel, eds., *RoboCup 2017: Robot World Cup XXI*. Springer International Publishing, Cham, pp. 290–301. ISBN 978-3-030-00308-1.

Fitzgerald, A., Kingsley, C.J. and Umans, S., 2003. *Electric Machinery*. McGraw-Hill, 6th edition.

Karnopp, D., Margolis, D.L. and Rosenberg, R.C., 2012. *System dynamics : modeling, simulation, and control of mechatronic systems*. Wiley, 5th edition.

Meessen, K., Paulides, J. and Lomonova, E., 2010. "A football kicking high speed actuator for a mobile robotic application". pp. 1659 – 1664. doi:10.1109/IECON.2010.5675433.

Oxley, P., Goodell, J. and Molt, R., 2009. "Magnetic properties of stainless steels at room and cryogenic temperatures". *Journal of Magnetism and Magnetic Materials - J MAGN MAGN MATER*, Vol. 321, pp. 2107–2114. doi:10.1016/j.jmmm.2009.01.002.

RoboCup, 2020. "Robocup soccer small size". `https://ssl.robocup.org/rules/`.

Zandsteeg, C., 2005. *Design of a RoboCup shooting mechanism*. DCT rapporten. Technische Universiteit Eindhoven. DCT 2005.147.

Zickler, S. *et al.*, 2009. "Cmdragons 2009 extended team description". Technical report, Carnegie Mellon University.

Zolanvari, A. *et al.*, 2015. "Parsian team description paper". Technical report, Electral Engineering Department, Amirkabir Univ. of Technology.

7. RESPONSIBILITY NOTICE

The authors are solely responsible for the printed material included in this paper.